Available online at www.sciencedirect.com

ScienceDirect

Procedia Structural Integrity 12 (2018) 204–212

Structural Integrity Procedia

www.elsevier.com/locate/procedia

AIAS 2018 International Conference on Stress Analysis

Numerical and experimental assessment of the static behavior of 3D printed reticular Al structures produced by Selective Laser Melting: progressive damage and failure

Franco Concli[a]*, Andrea Gilioli

[a]Free University of Bolzano/Bozen, piazza Università 1, Bolzano 39100, Italy

Abstract

In recent decades, the interest of the manufacturing industry towards additive manufacturing techniques has increased considerably. Speed and ease of implementation are just some of the factors that helped making this type of production one of the most developed in the world, considering also the possibility of creating complex geometries. The present research uses of a series of Al A357 specimens produced by SLM method. The experimental measurements on a first geometry have been used to calibrate the ductile damage model implemented in the FE code. The material model is based on both classical incremental model of plastic response with isotropic hardening and phenomenological concept of damage in continuum mechanic. The result of the calibration process was verified through the comparison of FE simulation of reticular specimens with the measured experimental response. Comparison between experimental data and numerical results will be discussed.

Keywords: Type your keywords here, separated by semicolons ;

1. Introduction

In recent years, the interest of the manufacturing industry towards additive manufacturing techniques has increased considerably. Speed and ease of implementation are just some of the factors that helped making this type

* Corresponding author. Tel.: +39-0471-017748; fax: +39-0471-017009
E-mail address: franco.concli@unibz.it

10.1016/j.prostr.2018.11.094

of production one of the most attractive. Its flexibility opens new possibilities in creating complex geometries such as reticular or lattice structures ensuring, for example, significant weight reductions or energy absorption capabilities. Among the different types of technology belonging to the additive manufacturing branch, selective laser melting (SLM) is the technique investigated in the present study.

In particular, a reticular structure is the sample analyzed in present research. Such kind of structure can ensure weight reductions without affecting the stiffness of the system. Furthermore, by acting on the morphological characteristics of the internal geometry, it is possible to modulate its mechanical response.

In this sense, several authors have proposed FE based approaches for the characterization of the behavior of an elementary cell subjected to external loads. Below the first yielding, the mechanical response of the elementary cell (Mahmoud Dalia 2017) can be simulated adopting simplified models based either on beams (Savio Gianpaolo, Gaggi Flavio, Meneghello Roberto 2015) or on an "equivalent solid material" which elastic properties depends from a density function (Hadi, n.d.).

Above the first yielding, while the "equivalent solid material" approach is no more able to predict the mechanical response of the lattice structure, the beam-based approach can still work properly up to the point in which internal contacts (between the beams themselves) take place.

As a consequence, the most reliable way to describe the behavior up to the final crushing point of a reticular structure is by means of a full-3D FE along with an adequate plasticity model and damage criterion. In present activity, an incremental model of plasticity with isotropic hardening and a ductile damage criterion with element deletion have been adopted. Even if this approach has been recognized as accurate (Gilioli et al. 2015), on the other hand, the computational times required for each simulations does not allow its extensive use for the direct design of real components.

In the first part of the work, the authors have calibrated the ductile damage model for an aluminum alloy A357 by means of round bar samples. Then in the second part, the model was successively applied to a different lattice structures for validation. The comparison has shown promising results.

2. Materials and methods

2.1. Material

The material adopted in this study is an A357 aluminum alloy. It has good fatigue and corrosion resistance properties (Es-Said et al. 2002). A357 produced by conventional technologies is generally strengthened by the precipitation hardening through a T6 heat treatment (530–540°C for 1–12 h followed by quenching in water at room temperature and artificial ageing at 150–225°C between 3 h and 6 h (Saboori et al. 2017)).

The required data for the FE analysis are the true stress-strain curve and the fracture locus. The first one is the key element for a reliable replication of the plastic behavior of the material whilst the second is fundament in the development of the damage criterion..

Experimental standard tensile tests were conducted on a MTS Criterion 45 testing machine up to the fracture.

Up to necking, the true stress-strain curve can be derived in a direct way from the measured loading-displacements diagram (continuous line in Figure 1b). The necking phenomena produces a non-uniform stress distribution in the cross section of the sample. An iterative method (numerically based) for plotting the stress-strain curve after necking should be adopted (Mae et al. 2007).

Bluhm and Morrissey (Bluhm J.I., Morrissey R.J., n.d.) suggested that the macroscopic crack formation takes place just before the load drop: the load-displacement peak can be identified as the instant in which the fracture starts. By combining experimental measurements on different sample geometries (different stress triaxiality) with FE simulations, it is possible to define the fracture locus. The fracture-start is individuated experimentally. FE simulations of such tests could provide the fracture strain (ε_{peq}) and the level of triaxiality (t) for the measured displacement to fracture (u_f).

The results should be then interpolated (Johnson and Cook 1983). Rice and Tracey (Rice and Tracey 1969) suggest to use an exponential function. Hancock and McKenzie (Hancock and Mackenzie 1976) propose a modified version of the Rice and Tracey model. Bao and Wierzbiki suggest that the fracture locus consist of three separate branches rather than a monotonic curve. More advanced models were proposed by Cortese et al (Cortese, Nalli, and Rossi 2016).

For this preliminary stage of the research, just one cylindrical sample geometry was available. It was used to validate numerically and experimentally the data found by Mae et al (Mae et al. 2007) for the same aluminium alloy (Figure 1a). The tests were performed on round samples. The fracture strain was found to be $\varepsilon_{peq} = 0.055$ when the level of triaxiality was $t = 0.38$. This observation fully confirm the data of Mae et al. Additional test are ongoing on different sample geometries to investigate also the left part of the fracture locus (low triaxiality below 0.33).

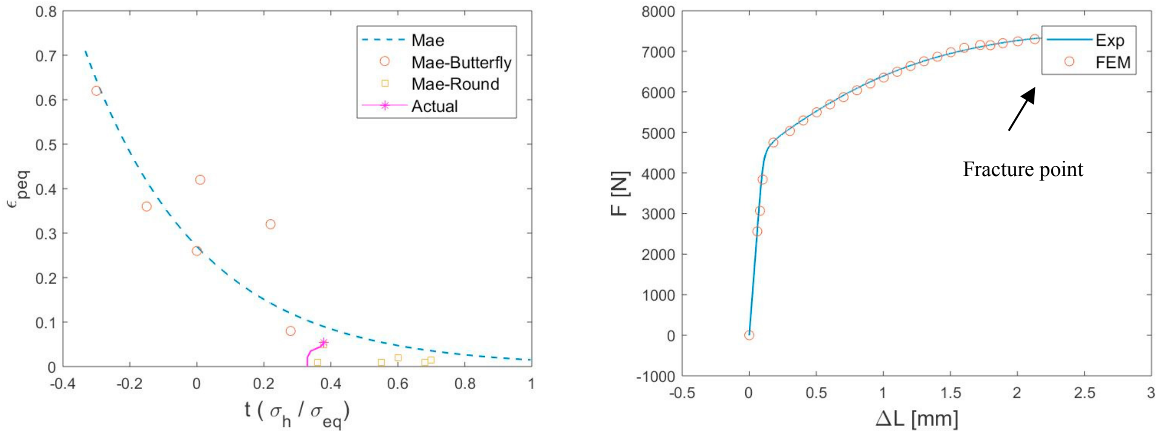

a) b)

Figure 1: mechanical properties of an A357 aluminum alloy: a) fracture strain vs. triaxiality (Mae et al. 2007); b) force-displacement measurements on the AM round samples

2.2. AM reticular samples

A series of A357 aluminum alloy specimens characterized by an internal reticular structure with Kagome cells were manufactured with the support of the Dept. of Mechanical Engineering of the Politecnico di Milano using a Renishaw AM250 selective laser melting system (SLM). The considered geometries are shown in Figure 2 and differ only in the diameter ϕ of the trusses (0.5 – 1.5 mm).

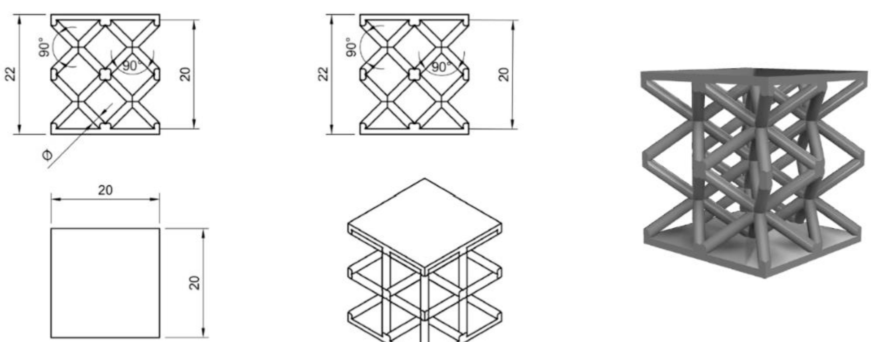

Figure 2: geometry of the adopted samples

2.3. Experimental tests on the reticula

Both geometries have been experimentally tested (compression) under quasi-static loading on a MTS Criterion 45 universal testing machine able to perform test up to 100 kN.

Tests were performed using dedicated compression plates (Figure 3) andthe samples were positioned in the middle of them. Tests were performed (displacement control of the upper plate) measuring the reaction force given by the sample. No extensiometer were mounted on the structure but it reasonable to assume that the displacement of the upper plate is representative of the compression of the samples which stiffness is much lower than the stiffness of the system itself. Each test was performed with a constant speed of 1mm/min to avoid dynamic effects. Two ripetitions were made for each reticular geometry.

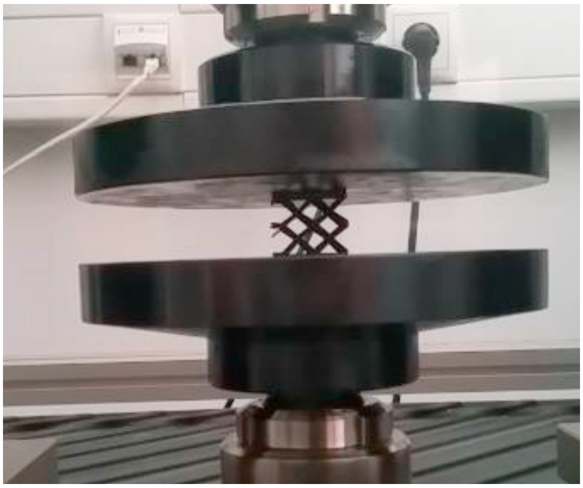

Figure 3: compression test

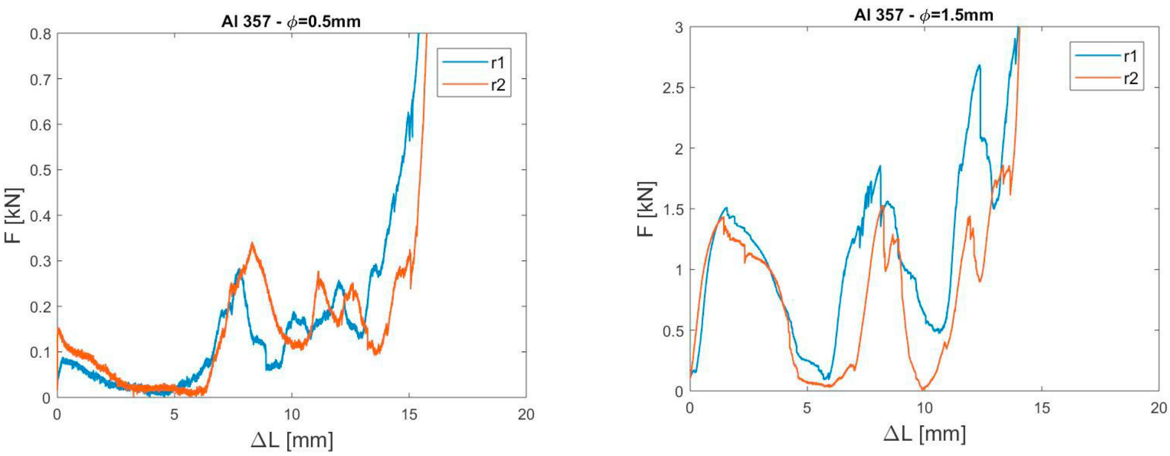

Figure 4: measured force-displacement curves for the two reticular geometries, r1 and r2 stand for the replication considered

From Figure 4, it can be observed that for such a material, the experimental results, especially for high ΔL, have a certain variability. This is related to the manufacturing technology which accuracy is limited and this can have a huge impact especially on such small structures. Furthermore, to reduce the level of porosity, HIP (Hot Isostatic

Pressing) treatments are strongly recommended while in this research the samples were tests as directly after their production.

2.4. Numerical simulations of the reticula

FE analysis were conducted in order to reproduce the macroscopic behavior of the specimens under compressive loads with the commercial software Abaqus (Concli et al. 2018). The two geometries were modeled taking advantage of the symmetry. Each model (Figure 5) was discretized with about 100k elements. The two plates were modeled with C3D8R (8-node linear bricks with reduced integration and hourglass control) elements while the trusses with C3D6 (linear triangular prisms) elements.

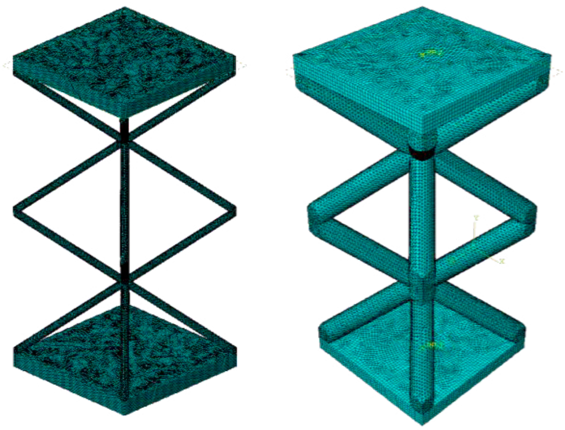

Figure 5: mesh details

FE simulations were performed with a dynamic explicit solver. The Johnson-Cook (Johnson and Cook 1983) damage model was uses to reproduce the ductile damage. In its general formulation it can be written as

$$\varepsilon_{peq} = [D_1 + D_2 \exp(D_3 \cdot t)][1 + D_4 \exp(\dot{\varepsilon}_p^*)][1 + D_5 \exp(T^*)] \quad (1)$$

In the present research, the fracture strain was assumed to be independent from the strain-rate and from the temperature (quasi static test at room temperature). Calibrating the Johnson-Cook model with the experimental data (Figure 1), the constants become $D_1 = 0$, $D_2 = 0.27$, $D_3 = -2.90$, $D_4 = 0$ and $D_5 = 0$.

The stress-strain response will show distinct phases. The material response is initially linear elastic, followed by plastic yielding with strain hardening. Beyond this point, there is a marked reduction of load-carrying capacity until rupture. The deformation during this last phase is localized in a neck region of the specimen. This point identifies the material state at the onset of damage, which is referred to as the damage initiation criterion (Johnson-Cook). Beyond this point, the stress-strain response is governed by the evolution of the degradation of the stiffness in the region of strain localization. Practically, after this point is damaged in an irreversible way therefore if unloaded the response has no longer the undamaged stiffness but a lower value.

$$\bar{\sigma} = \frac{F}{A - A_D} = \frac{\sigma}{1 - D} \quad (2)$$

$$\sigma = E_0 (1 - D)\varepsilon \quad (3)$$

where A is the original surface area, A_D the defects surface area, F the external load, $D = A_D / A$ the damage evolution and E_0 the elastic module. It describes the rate of degradation of the material stiffness once the corresponding initiation criterion has been reached. As the element reaches a prescribed level of degradation ($D = 1$), elements may be removed from the mesh.

In continuum mechanics, the constitutive model is normally expressed in terms of stress-strain relations. When the material exhibits strain-softening behavior, leading to strain localization, this formulation results in a strong mesh dependency of the finite element results in that the energy dissipated decreases upon mesh refinement. In the adopted FE software, the damage evolution models use a formulation intended to alleviate the mesh dependency. The law proposed by Hooputra et al (Hooputra et al. 2004) is accomplished by introducing a characteristic length into the formulation, which is related to the element size, and expressing the softening part of the constitutive law as a stress-displacement relation ($\bar{u}_f = L \cdot \bar{\varepsilon}_{peq}$ where $\bar{\varepsilon}_{peq}$ is the equivalent plastic strain and L the characteristic length of the finite element (Ribeiro J, santieag A 2016)).

3. Results

Figure 6 shows the comparison between the numerical simulation results and the experimental data. The simulation reproduce, compatibly with the statistical variance of the measured data, both the peaks positions as well as their magnitude. The prediction are more accurate for the samples with a truss diameter of $\phi = 1.5mm$. This is due to the fact that the same surface quality (porosities, roughness etc.), function of the manufacturing process, has a lower impact for bigger parts resulting in more stable measurements.

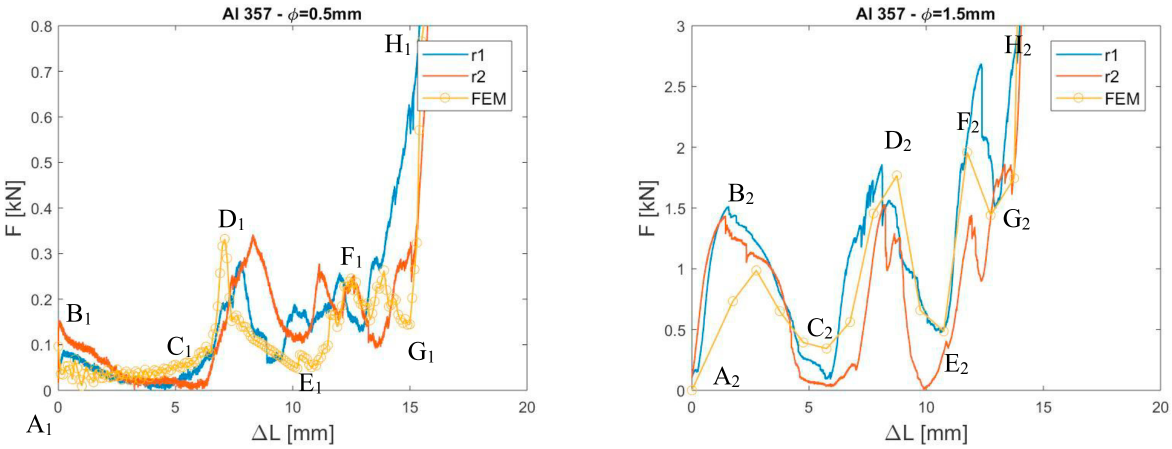

Figure 6: F-ΔL: comparison between simulated and measured data

In the reticula with the smallest truss diameter ($\phi = 0.5mm$), after a first phase in which the structure behaves in a purely elastic manner (A_1-B_1), the trusses of the intermediate row start to deform due to instability. This produce a sudden decrease of the stiffness of the reticula. The minimum value is reached in C_1 where the intermediate "hinges" (Figure 7) start to plasticize. This phase (C_1-D_1) produce an increase in the stiffness due to hardening. The three steps are then repeated for the other two rows of the reticula. In F_1, instability takes place causing a decrease of the stiffness. Then a plastic phase start (F_1-G_1). In G_1, the upper and lower "hinges" (Figure 7) are completely deformed but still attached. From G_1 to H_1, the sudden increase in the reaction force is due to the complete packing of the structure.

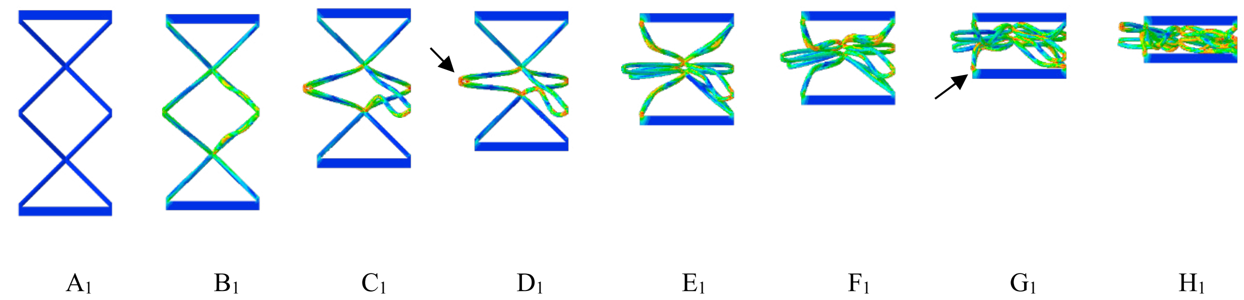

Figure 7: progressive damage of the thinnest reticula, letters refer to Figure 6

The second reticula, in which the truss diameter is $\phi = 1.5mm$, behaves differently because instability plays a lower role. The first elastic part (A_2-B_2) is much more extended. Instability takes place only after 2 mm of ΔL (for the thinner reticula after only 0.1mm). The second peak, associated with the end of the elastic phase of the upper and lower rows of trusses, shows, as expected, a higher value with respect to the first one. This is due to the fact that the stiffness of the intermediate row is lower due to the different geometrical configuration (full Kagome cell vs. half Kagome cell). After D_2, the decrease of the load is not due to the instability of the trusses but due to the fracture of the material in correspondence of the upper hinges (Figure 8) (detachment of the trusses from the plates). The same happens in F_2 for the lower connections. From G_2 to H_2 the sudden increase in the reaction force is due to the complete packing of the structure.

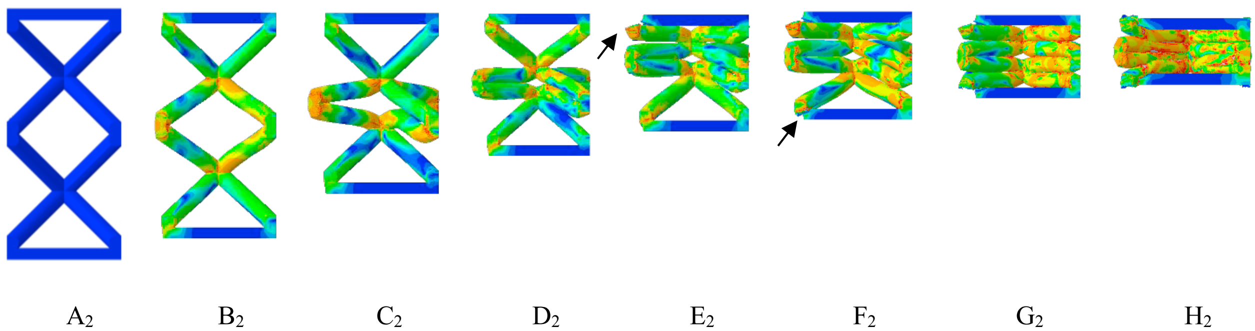

Figure 8: progressive damage of the thickest reticula, letters refer to Figure 6

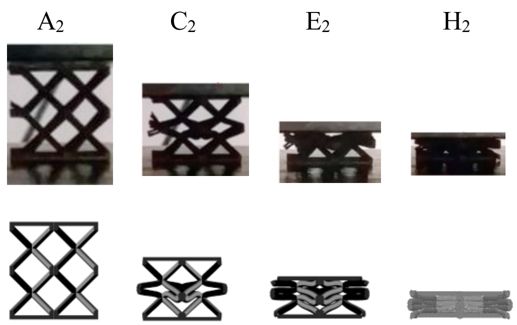

Figure 9: progressive deformation of the thickest reticula, letters refer to Figure 6

4. Performance enchantments

Simulations were performed on a 76.8GFLOPS workstation. Each simulation took approximatively 30 h.

5. Future work

A wide testing campaign is ongoing in order to better characterize the mechanical properties of the A357 aluminum alloy. Despite the Johnson-Cook model for ductile damage tuned with the constants provided by Mae et al has ensured promising results, additional works has to be made to better understand the relation between fracture strain and parameters such as triaxiality, Lode angle etc..

Furthermore, the high computational effort of the adopted numerical approach is a limiting factor to the direct application of this methodology to design of reticular/lattice structures.

The authors plan to simulate the F_i-ΔL_i and T_i-$\Delta\varphi_i$ relations for the different elementary cells. One such relation are defined, the behavior of a single cell can be described with 6 simple springs allowing the simulation of much more complex systems in which thousands of elementary cells are present.

6. Conclusions

In the present paper, a preliminary study was made on order to characterize the stiffness of a double Kagome reticular structure made of an A357 aluminum alloy.

A first test on a round bar was made in order to validate the fracture locus proposed by Mae et al. (Mae et al. 2007) for the considered aluminum alloy. The test shows a fracture strain $\varepsilon_{peq} = 0.055$ in correspondence to a level of triaxiality $t = 0.38$. This is in accordance with the findings of Mae et al. Mae's constants were used to define the fracture locus (Johnson-Cook model) for the FE simulations.

Two reticular structures, characterized by different truss diameters ($\phi = 0.5 \div 1.5mm$), were experimentally tested (compression) and numerically simulated. Measurements show a large scatter related to the low manufacturing quality. The simulation results are aligned with the measurements.

The failure mechanisms of the two structures is slightly different. While in the thinner structure instability plays a fundamental role, in the ticker structure this phenomena is negligible.

References

Bluhm, J.I., Morrissey, R.J., Yokobori, T., 1966. In Conf. Fracture.

Concli, F., Cortese, L., Vidoni, R., Nalli, F., Carabin, G., 2018. "A Mixed FEM and Lumped-Parameter Dynamic Model for Evaluating the Modal Properties of Planetary Gearboxes." Journal of Mechanical Science and Technology 32 (7): 3047–56.

Cortese, L., Nalli, F., Rossi, M., 2016. "A Nonlinear Model for Ductile Damage Accumulation under Multiaxial Non-Proportional Loading Conditions." International Journal of Plasticity 85: 77–92.

Es-Said, O.S., Lee, D., Pfost, W.D., Thompson, D.L., Patterson, M., Foyos, J., Marloth, R., 2002. "Alternative Heat Treatments for A357-T6 Aluminum Alloy." Engineering Failure Analysis 9 (1): 99–107.

Gilioli, A, Manes, A., Giglio, M., Wierzbicki, T., 2015. "Predicting Ballistic Impact Failure of Aluminium 6061-T6 with the Rate-Independent Bao-Wierzbicki Fracture Model." International Journal of Impact Engineering 76: 207–20.

Azman A.H, 2018. "Method for Integration of Lattice Structures in Design for Additive Manufacturing." Université Grenoble Alpes.

Hancock, J.W., Mackenzie, A.C., 1976. "On the Mechanisms of Ductile Failure in High-Strength Steels Subjected to Multi-Axial Stress-States." Journal of the Mechanics and Physics of Solids 24 (2–3): 147–60.

Hooputra, H., Gese, H., Dell, H., Werner, H., 2004. "A Comprehensive Failure Model for Crashworthiness Simulation of Aluminium Extrusions." International Journal of Crashworthiness 9 (5): 449–63.

Johnson, G.R., Cook, W.H., 1983. "A Constitutive Model and Data for Metals Subjected to Large Strains, High Strain Rates and High Temperatures." A Constitutive Model and Data for Metals Subjected to Large Strains, High Strain Rates and High Temperatures, 541–47.

Mae, H., Teng, X., Bai, Y., Wierzbicki, T., 2007. "Calibration of Ductile Fracture Properties of a Cast Aluminum Alloy." Materials Science and Engineering: A 459 (1): 156–66.

Mahmoud, D., Elbestawi, M.A., 2017. "Lattice Structures and Functionally Graded Materials Applications in Additive Manufacturing of

Orthopedic Implants: A Review.” Journal of Manufacturing and Materials Processing 1 (13).
Ribeiro J., Santieag, A., Rigueiro, C., 2016. “Damage Moel Calibration and Application for S355 Steel.” In Procedia Structural Integrity. Elsevier.
Rice, J.R, Tracey, D.M., 1969. “On the Ductile Enlargement of Voids in Triaxial Stress Fields*.” Journal of the Mechanics and Physics of Solids 17 (3): 201–17.
Saboori, A., Pavese M., Badini C., Eivani A.R., 2017. “Studying the Age Hardening Kinetics of A357 Aluminum Alloys through the Johnson–Mehl–Avrami Theory.” Metal Powder Report 72 (6): 420–24.
Savio G., Gaggi F., Meneghello R., Concheri G., 2015. “Design Method and Taxonomy of Optimized Regular Cellular Structures for Additive Manufacturing Technologies.” In ICED.